The interface ionic liquid(s)/electrode(s): *In situ* STM and AFM measurements

Frank Endres,*[ab] Natalia Borisenko,[ab] Sherif Zein El Abedin,[abc] Robert Hayes[d] and Rob Atkin[d]

Received 30th March 2011, Accepted 13th April 2011
DOI: 10.1039/c1fd00050k

The structure of the interfacial layer(s) between the extremely pure air- and water-stable ionic liquid 1-butyl-1-methylpyrrolidinium tris(pentafluoroethyl) trifluorophosphate and Au(111) has been investigated using *in situ* scanning tunneling microscopy (STM) at electrode potentials more positive than the open circuit potential. The *in situ* STM measurements show that layers/islands form with increasing electrode potential. According to recently published atomic force microscopy (AFM) data the anion is adsorbed even at low anodic overvoltages and adsorption becomes slightly stronger with increasing electrode potential. Furthermore, the number of interfacial layers increases with increasing electrode potential. The present discussion paper shows that these layers are not uniform and have a structure on the nanoscale, supporting earlier results that the interface electrode/ionic liquid is highly complex. It is also shown that the addition of solutes changes this structure considerably. AFM results reveal that in the pure liquid, interfacial layers lead to a repulsive force but the addition of 10 wt% of LiCl leads to an attractive force close to the surface. These preliminary results show that solutes strongly alter the interfacial structure of the ionic liquid/electrode interface.

Introduction

Ionic liquids (ILs) have attracted considerable research interest in surface science and in physical chemistry in recent years. Apart from wide electrochemical and thermal windows they have high ionic conductivities, acceptable viscosities and extremely low vapor pressures. The latter properties make them suitable for ultra-high vacuum studies, and their wide electrochemical windows of up to ± 3 V *vs.* NHE (including thermodynamic and kinetic contributions) are attractive for electrochemistry. The prospects and challenges of ILs in the field of electrochemical energy science were discussed in.[1] The interface of diluted electrolyte solutions/electrodes is usually described by the Helmholtz model, the Gouy-Chapman model, and the Stern model, the latter being more or less a combination of the first two. The measurable double layer capacitances of aqueous electrolytes/electrodes are around 100 μF cm^{-2}, and usually have a minimum at the potential of zero charge. For a description of ionic liquids/electrodes one has to bear in mind that these models were developed for dilute electrolytes, thus application to ILs which have a high density of positive

[a]*Institute of Particle Technology, Clausthal University of Technology, Arnold-Sommerfeld-Strasse 6, 38678 Clausthal-Zellerfeld, Germany. E-mail: frank.endres@tu-clausthal.de*
[b]*EFZN Goslar, Am Stollen 19, 38640 Goslar, Germany*
[c]*Electrochemistry and Corrosion Laboratory, National Research Centre, Dokki, Cairo, Egypt*
[d]*Centre for Organic Electronics, Chemistry Building, The University of Newcastle, Callaghan, New South Wales, 2308, Australia. E-mail: Rob.Atkin@newcastle.edu.au*

and negative charges is not appropriate. An IL represents a dense system of cations and anions with no solvent, so that the individual interactions between neighbouring ions cannot be neglected.[2–4] Thus, for ILs the situation is much more complicated. Several groups studied the double layer behaviour of ILs. Lockett *et al.* demonstrated hysteresis effects in the differential double layer capacitance, as well as maxima and minima in the capacitance curve, referred to as the *camel shape* capacitance curve.[5] Similar results were presented in reference 6 and Fedorov and Kornyshev suggested a theoretical model, which explains the results:[7] at an open circuit potential both the charged groups and neutral groups (chains) on the ions interact with the electrode surface. With increasing cathodic or anodic electrode potentials a reorientation occurs with the neutral groups repelled from the surface and replaced by the ion charged groups. Consequently an increase in double layer capacitance results until saturation is reached at high electrode potentials. This model was further developed and quite a recent theoretical study shows that ion multilayers can be described.[8] This is consistent with previous AFM[9] and X-ray[10] reflectivity measurements that revealed ILs are strongly adsorbed on solid surfaces and that several layers are present adjacent to the surface. In a joint paper we (Atkin and Endres *et al.*) showed that 1-butyl-1-methylpyrrolidinium bis(trifluoromethylsulfonyl) amide and 1-ethyl-3-methylimidazolium bis(trifluoromethylsulfonyl)amide behave quite differently on Au(111). Both liquids are adsorbed at the open circuit potential but the first one approximately 4 times more strongly.[11] It should be mentioned that the adsorption of ILs on a solid surface is not at all surprising as water and organic solvents can also be adsorbed.[12–14] However, the force to rupture IL layers is quite surprising as it is one order of magnitude higher than for aqueous/organic solvents. Such a strong adsorption must influence the image quality in an *in situ* STM experiment.[15] In a recently published joint paper the structure and dynamics of the interfacial layers between the air- and water-stable IL 1-butyl-1-methylpyrrolidinium tris (pentafluoroethyl)trifluorophosphate ($[Py_{1,4}]$FAP) and Au(111) were investigated using STM, cyclic voltammetry (CV), electrochemical impedance spectroscopy (EIS), and AFM measurements. *In situ* STM measurements reveal that the Au (111) surface undergoes a reconstruction, and at −1.2 V (*vs.* Pt quasi-reference) the $(22 \times \sqrt{3})$ "herringbone" superstructure is probed. AFM force–distance profiles showed that the IL becomes more structured at higher cathodic potentials and both the number of detectable layers and the push-through forces increase. EIS measurements showed a capacitive process at the IL/Au(111) interface which is considerably slower than electrochemical double layer formation and seems to be related to the herringbone reconstruction of Au(111).[16] It should be mentioned that the interface (electro-)chemistry of ILs is altered by solutes and even low amounts of impurities can have a considerable effect.[17] In the present paper we focus on *in situ* STM experiments in the anodic regime of $[Py_{1,4}]$FAP/Au(111). It will be shown that structures form on the nanoscale for electrode potentials of up to +2 V *vs.* the open circuit potential (ocp). These structures disappear when the electrode potential is returned to the ocp, and the original surface is recovered. Thus, the observed processes on the surface are reversible and not due to impurities which in this liquid are all below 10 ppm. Preliminary AFM results show that the addition of 10 wt% of LiCl strongly alters the near surface structure and in contrast to repulsive forces measured for the pure IL-interfaces (see references 18–20) the AFM tip experiences attractive forces on approach to the gold surface.

Experimental

1-Butyl-1-methylpyrrolidinium tris(pentafluoroethyl)trifluorophosphate ($[Py_{1,4}]$FAP) was purchased from Merck in the highest available quality. The liquid was custom-made and the purity protocol delivered by Merck showed that all detectable impurities were below 10 ppm. HF and oxide levels were below the detection limit of 10 ppm. It is important to mention that impurities in ILs, which are often present in

commercial ILs (even in apparently ultrapure quality), can strongly alter the surface processes easily leading to misinterpretations.[17] There can be numerous impurities including decomposition products of anions and/or cations, side products from synthesis, Li^+, Na^+, K^+, and halides in the 1000 ppm range even in apparently ultrapure ILs. Even worse, purification procedures may introduce SiO_2 or Al_2O_3 particles.[21] Prior to use we analyze all ILs using CV, XPS and *in situ* STM to ensure the purity. If there are metallic impurities they are usually detected by STM on Au(111) in the cathodic regime and by underpotential deposition processes visible in the cyclic voltammogram. We should mention that a definite exclusion of impurities is quite challenging and needs the combination of several techniques together with a good amount of experience. Therefore, for fundamental studies we require custom-made ILs of the highest possible purity to avoid misinterpretations. Additionally our liquids are dried under vacuum (10^{-3} mbar) at 100 °C to H_2O contents of well below 1 ppm and stored in a closed bottle in an Ar-filled glove box with H_2O and O_2 contents of below 2 ppm (OMNI-LAB from Vacuum-Atmospheres). *In situ* STM and AFM measurements were carried out using samples of the same IL which were sent in sealed ampoules to the Newcastle group. The substrates for AFM and STM experiments and the working electrode (WE) were Au(111) (a 300 nm thick film on mica) purchased from Agilent. Directly before use, the substrates were carefully heated in a H_2-flame to minimize possible surface contaminations. CV measurements were carried out in the glove box using a Parstat 2263 potentiostat/galvanostat (Princeton Applied Research) controlled by a PowerCV software. The electrochemical cell was made of polytetrafluoroethylene (Teflon) and clamped over a Teflon-covered Viton O-ring onto the substrate, thus yielding a geometric surface area of the WE of 0.3 cm^2. Pt wires (Alfa Aesar, 99.99%) of 0.5 mm diameter were applied as quasi-reference (RE) and counter (CE) electrodes, respectively. From our experience, Pt has a sufficiently stable electrode potential under *in situ* STM/AFM conditions. Directly before use the Pt wires were cleaned for 15 min in an ultrasonic bath in acetone followed by heating in a H_2-flame to red glow for a few minutes to minimize surface contaminations.

LiCl was sourced from Sigma-Aldrich (99%) and dried in a vacuum oven at 100 °C for 24 h prior to use. AFM force measurements were acquired continuously using a Digital Instruments NanoScope IIIa Multimode AFM in contact mode in an incubator at 21 °C. The scan rate and scan size were kept between 0.1 and 0.5 Hz and 10 and 50 nm, respectively. The Si_3N_4 cantilever was carefully rinsed in Milli-Q H_2O, dried and irradiated with ultraviolet light for 40 min prior to use. The IL was held in an AFM fluid cell, sealed using a silicone O-ring. Both of these were cleaned by sonication for 30 min, rinsed copiously in distilled ethanol and Milli-Q H_2O, and then dried using filtered N_2. A modified AFM cell setup was used to acquire force curves as a function of potential. A thin cylindrical strip of Cu metal and 0.25 mm Pt wire were used as the CE and RE, respectively. The CE and RE were cleaned firstly in diluted HCl acid solution and then washed with distilled ethanol and Milli-Q H_2O and dried using filtered N_2. The CE was mounted with the O-ring in the groove of the fluid cell to establish an equipotential WE surface. The RE was located directly above the centre of the WE surface by securing the Pt wire through the outlet valve of the fluid cell. The electrodes were connected to an EG & G Princeton Applied Research Model 362 Scanning Potentiostat.

The features of the AFM force curves at a given surface potential did not alter over a 48 h period. Typical start distances for force scans were 30–50 nm from the Au(111) surface. The maximum applied force in contact was between 30 and 500 nN.

STM experiments were performed at 23 °C using in-house-built STM heads and scanners under inert gas conditions (H_2O and O_2 < 2 ppm) with a Molecular Imaging PicoScan 2500 STM controller in feedback mode. Assembling of the STM head and filling of the electrochemical cell were performed in an Ar-filled glove box solely reserved for assembling of STM heads. The STM head was placed inside an Ar-filled vacuum-tight stainless steel vessel, to ensure inert gas atmosphere during

the STM experiments, transferred to the air-conditioned laboratory ($T = 23 \pm 1$ °C) and placed onto a vibration damped table from IDE (Germany). STM tips were made by electrochemical etching of Pt-Ir wires (90/10, 0.25 mm diameter) with a 4 mol L^{-1} NaCN solution and subsequently electrophoretically coated with an electropaint (BASF ZQ 84-3225 0201). During the STM experiments the potential of the WE was controlled by the PicoStat from Molecular Imaging/Agilent.

Results and discussion

Before presenting new *in situ* STM results we will first review the cyclic voltammograms and our previous STM/AFM data on the interface structure of Au(111) in [$Py_{1,4}$]FAP in the cathodic regime to provide context. For details we refer the reader to references 16 and 22. Fig. 1 shows the cyclic voltammogram of Au(111) in [$Py_{1,4}$]FAP at a scan rate of 10 mV s^{-1} between −3 and +1 V *vs.* the Pt quasi reference electrode. This voltammogram remains stable for subsequent scans and in[16] we showed that the cathodic peaks C1–C4 and their anodic counterparts are not due to Faradaic reactions. The AFM data presented in reference 16 show that there is a cation-rich layer with a thickness of 0.35 nm at the ocp. At −1 V the cation-rich layer is 0.25 nm thick and in both cases several layers of ionic liquid are on top of this layer. At −2 V the cation is so strongly adsorbed that it cannot be displaced by the AFM tip, and only an anion layer is detected. STM at the ocp shows a more or less normal terraced Au(111) surface. With decreasing electrode potential the herringbone superstructure is probed; this structure disappears at more negative electrode potentials. *In situ* STM did not give a clear picture of the adsorbed IL layers but did reveal restructuring of the gold surface. Fig. 2 shows the cyclic voltammogram of Au(111) in [$Py_{1,4}$]FAP at a scan rate of 10 mV s^{-1} between −3 and +2 V *vs.* the Pt quasi reference electrode. The current response between −3 and +1 V is almost identical to the CV presented in Fig. 1. At electrode potentials of above 1 V the current remains almost constant and starts to rise steeply with a shoulder at ∼ +1.5 V. In the backscan 2–3 cathodic waves are observed between ∼ +0.8 and −0.2 V. The steeply rising anodic current up to +2 V is difficult to allocate to a reaction. In the STM experiments described in more detail below we lost the contrast at +2 V but there were no definite hints for gold oxidation. Therefore we might conclude that this anodic reaction is mainly due to an oxidation of the IL. Only at higher electrode potentials of up to +3 V on this scale we observed the oxidation of gold. The cyclic voltammogram alone implies a featureless surface electrochemistry in the anodic regime whereas in the cathodic regime definite processes

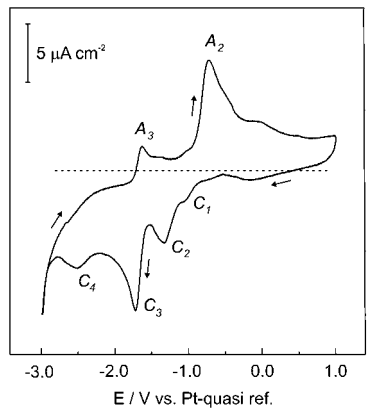

Fig. 1 Cyclic voltammogram of Au(111)/[$Py_{1,4}$]FAP at a scan rate of 10 mV s^{-1} between −3 V and +1 V (see also reference 16).

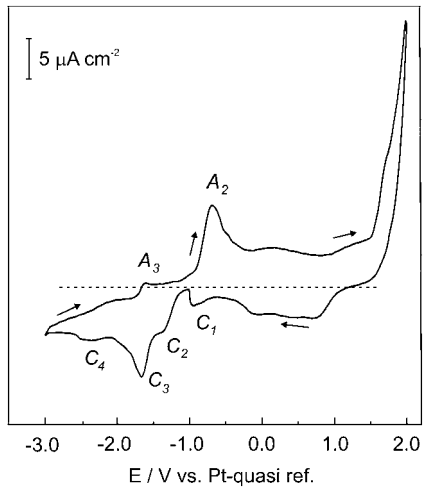

Fig. 2 Cyclic voltammogram of Au(111)/[$Py_{1,4}$]FAP at a scan rate of 10 mV s^{-1} between −3 V and +2 V.

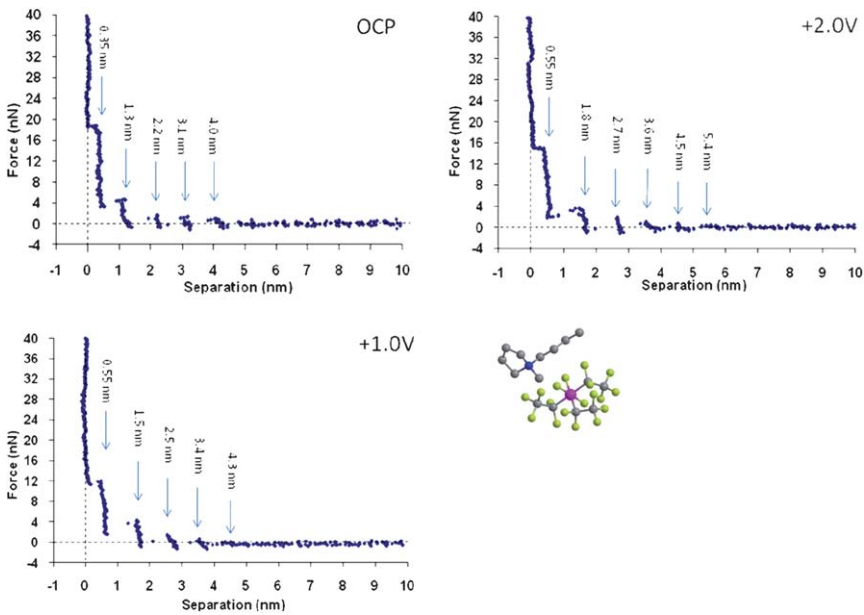

Fig. 3 AFM force/distance profiles of Au(111)/[$Py_{1,4}$]FAP in the anodic regime, from reference 22. At the ocp cation adsorption prevails whereas with more anodic electrode potentials a preferential anion adsorption sets in.

are observed. Fig. 3 shows AFM approach curves at open circuit potential, +1 V and +2 V *vs.* the Pt quasi reference electrode.[22] As there is a negligible Faradaic process, the composition of the electrolyte is not altered, thus the reference electrode is stable. At the ocp there are 5 layers. Beginning 4 nm from the surface there are 4 steps each 0.9 nm, consistent with the size of the ion pair. The last layer, however, is only 0.35 nm thick indicative of the layer in contact with the surface being enriched in the cation. According to Fig. 3 the interface structure changes when more positive

electrode potentials are applied. At + 1 V five layers are detected and the layer closest to the surface is 0.55 nm thick, indicative of anion adsorption. At +2 V the situation is similar, but the adsorbed anion layer appears slightly compressible. The AFM data alone would lead to the conclusion that these layers are more or less uniform, as the AFM tip probes reproducibly the same layer structure. The situation is slightly more complicated as our recent *in situ* STM results will show in this manuscript. In the past we mainly focused on the cathodic regime. On the one hand this is a consequence of our activities in the field of metal and semiconductor deposition, but on the other hand because the quality of the STM images in the anodic regime is usually lower. In the present study liquids of the highest available quality are used, allowing confidence that the observed surface modifications are due to the ionic liquid and not due to impurities. Fig. 4a shows a typical Au(111) surface in contact with $[Py_{1,4}]FAP$ with the typical terraces and 250 pm high steps at the open circuit potential. Zooming in does not give a better resolution and the images get rather blurred, which is a hint at the interaction of the STM tip with the surface. The AFM data show that there are at least 5 well-formed layers adjacent to the surface, and the layer closest to the surface is enriched in the cation and requires a push-through force of 20 nN, which is quite a high binding force. Nevertheless, electrons tunnel between the STM tip and surface, through this interfacial layer; the electronic structure in this layer will also determine exactly what the STM tip probes. As the typical distance between tip and sample in an STM experiment is 0.2–1 nm, the STM tip must move laterally through these adsorbed layers, meaning that ions are pushed away laterally. This — in our opinion — leads to the "blurred" image quality we often observe with these liquids. As these interfacial layers vary with liquid and electrode potential a simplification and a prediction for other liquids is not possible. There might be liquids that are much less strongly adsorbed allowing higher quality images to be obtained. We also expect that even low water concentrations will have an influence on these layers and thus alter the STM image quality. Fig. 4b shows the same site at +0.2 V (ocp + 0.4 V). Apart from a slight thermal drift the surface looks quite similar but is slightly rougher. Zooming in (Fig. 4c) shows

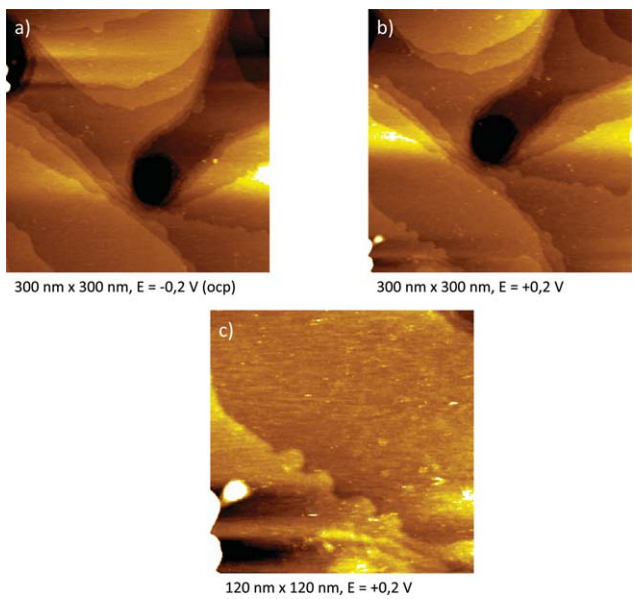

Fig. 4 *In situ* STM images of Au(111)/$[Py_{1,4}]FAP$ at ocp and at slightly more positive electrode potentials (ocp + 0.4 V). There is a layer on the surface and islands evolve.

clearly a layer on the surface and the step between 2 terraces (arrow) looks "buried". In the case of aqueous solutions such image quality would strongly hints for organic contaminations which makes an atomic resolution experiment very difficult. Fig. 5a shows the same site with 300 nm × 300 nm resolution at +0.5 V (ocp + 0.7 V). In comparison to Fig. 4a there are now more islands visible and a 120 nm × 120 nm image reveals a layer on the surface with some structure. The measured height differences between these islands is between 0.2 and 0.5 nm, but for reasons discussed above, the error in these values is quite high. The surface structure does not vary appreciably between +0.5 and +1.2 V but Fig. 6a shows a layer with islands on top at 1.2 V. Because of the poor image contrast the steps are less clearly visible than at −0.2 V (Fig. 4a). The islands on the surface are sharper on the 120 nm × 120 nm scale, *cf.* Fig. 6b, but the steps between the terraces remain "buried". The surface is not uniform, but 0.3–0.6 nm high islands can be distinguished as indicated by the arrow. The AFM data in Fig. 3 show that at this electrode potential a slightly compressible anion-rich layer is present. The force to rupture this layer is 12 nN which is also fairly high.

Given that there is a cation-rich layer adsorbed at the ocp and an anion layer at +1 and +2 V there must be a transition between these states. We believe that Figs. 4–6 show this transition. At the first glance it is surprising that the AFM gives more or less discrete signals whereas the STM shows a structured surface. However, these results are not inconsistent as the maximum height differences observed (*e.g.* in Fig. 6b) are not more than 0.5 nm which is significantly less than the dimension of the ion pair. It is possible that the non-vertical force signals in Fig. 3 are due to the non-uniformity of the surface observed by the STM, in accordance with previous results.[18] Figs. 7a and 7b show the Au(111) surface at +1.6 and +1.7 V. Compared to +1.2 V the surface is more uniform and smoother, and the islands have almost completely disappeared. Steps are less clearly visible than at ocp which is a strong indication of an adsorbed layer, but can be seen more clearly when the image size is reduced to 120 nm × 120 nm, *cf.* Fig. 7c, where the measurable height contrast is less than 0.1 nm. This situation does not change when the electrode potential approaches +2 V where, however, the contrast is lost which hints at an electrochemical reaction. According to the AFM data there is a slightly compressible adsorbed layer of the anion at this potential on top of which 4 ionic liquid layers lie. As the maximum height differences observed with the STM were ≈ 0.5 nm, and as the STM tip is positioned between 0.5 and 1 nm above the surface (independently determined by current/distance tunneling spectroscopy), we believe that the STM probes this anion-rich layer. It should be noted that the IL layer on top of this anion-rich layer still requires a force of 4 nN to rupture. Together these layers are 1.5 nm thick which is a considerable distance for the STM tip to penetrate.

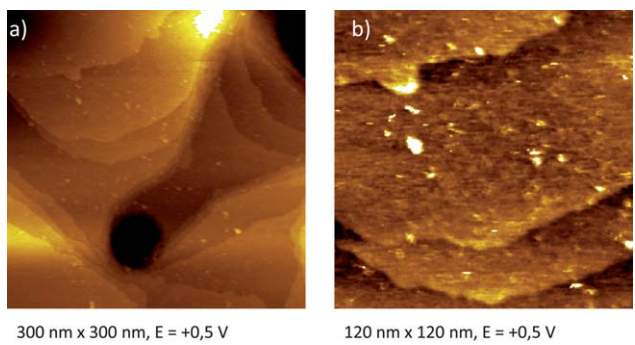

Fig. 5 *In situ* STM images of Au(111)/[$Py_{1,4}$]FAP at ocp + 0.7 V. The evolving islands become more visible.

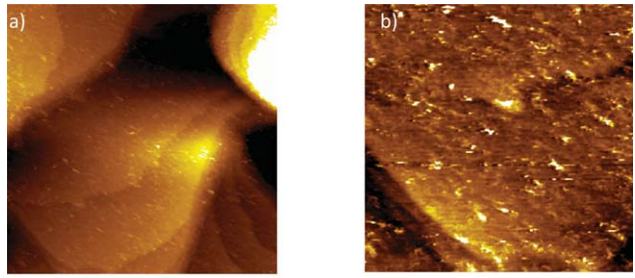

Fig. 6 *In situ* STM images of Au(111)/[$Py_{1,4}$]FAP at ocp + 1.4 V. The number of islands increases and the probed layer is not uniform.

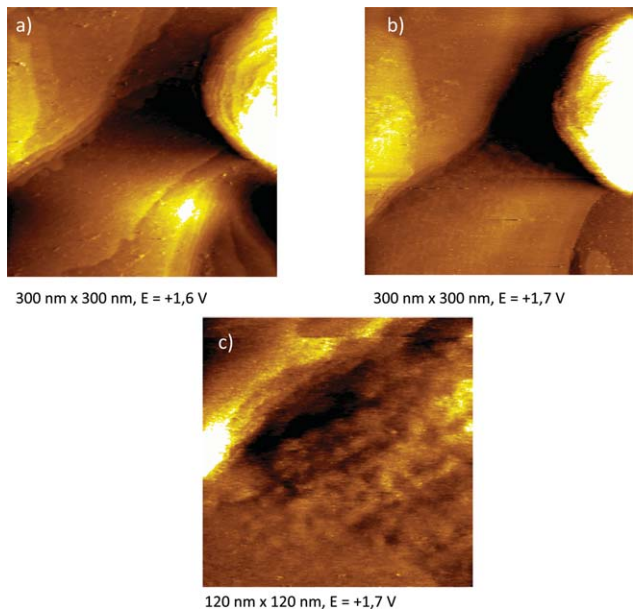

Fig. 7 *In situ* STM images of Au(111)/[$Py_{1,4}$]FAP at ocp + 1.8 V (a) and at ocp + 1.9 V. The terrace steps look "buried" and the layer shows a slight contrast with height differences of ≈ 0.1 nm.

Adsorption of cations and anions to the STM tip is also expected, which also reduce the image quality and force resolution. Nevertheless we think that the STM probes the real surface, *i.e.* the anion and the IL layers.

Electrochemical reactions at this potential will require that the interfacial IL structure is disrupted to allow the reactant to make contact with the electrode surface. In the following we reduced the electrode potential from +1.8 V to +1.5 V (Fig. 8a) and subsequently from +1.5 V to +1.2 V (Fig. 8b) then we left the electrode potential at +1.2 V for 20 min on the 300 nm × 300 nm scale (Figs. 8c–d). There is still a layer on the surface but the steps become more visible, with some islands noted on the gold surface. The measurable height difference is between 0.1 and 0.2 nm, thus, an allocation to cation or anion is hardly possible. Figs. 9a and 9b show on the 200 nm × 200 nm scale that the surface very slowly changes. The gold surface is difficult to probe in high quality and according to the AFM data adsorption leads to the

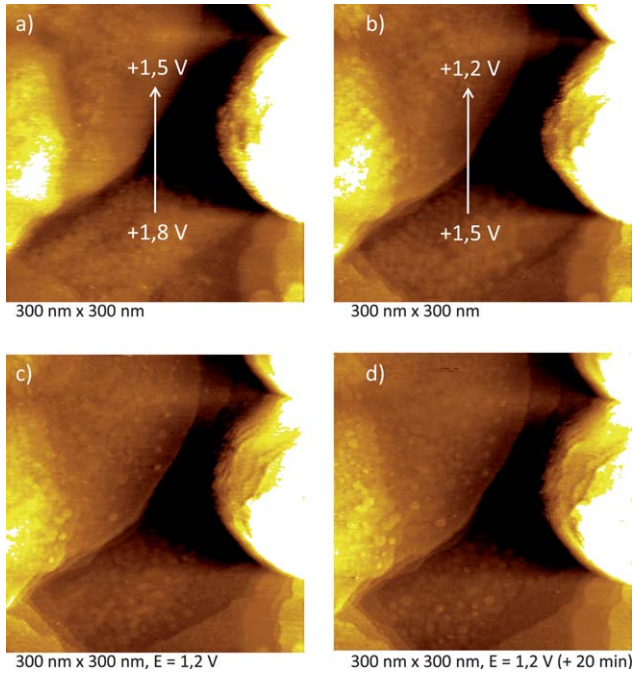

Fig. 8 *In situ* STM images of Au(111)/[$Py_{1,4}$]FAP: The electrode potential has been set to less positive values and islands with a height difference of $\approx$ 0.2 nm appear on the surface. This is indicative of a reorientation and hints at cations being involved.

interfacial layer being enriched in the anion. We cannot allocate the islands to cation/anion or an IL layer, but it can be concluded that the surface is non-uniform. There is no contradiction with the AFM data, as the height variation of 0.1–0.2 nm is beyond the resolution of the AFM experiment. It is therefore possible that the slight compressibility measured in the AFM curve is due to surface inhomogenity. Fig. 10 shows the surface of Au(111) at the former ocp, and the individual terraces are again clearly visible on the 300 nm $\times$ 300 nm scale. There are some horizontal stripes in the STM image which disappear with time. We do not believe that these

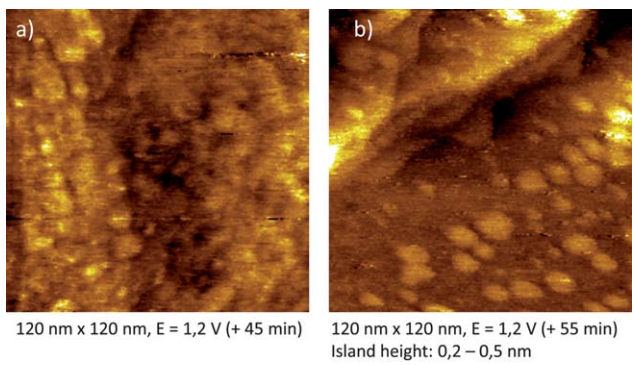

Fig. 9 *In situ* STM images of Au(111)/[$Py_{1,4}$]FAP. The surface very slowly changes (within hours) and is not probed in high quality. The adsorbed layer might disturb the tunneling process.

stripes are due to a bad tip, rather we think that the very slow reorientation of the surface leads to these blurred images. The images presented here were reproduced in several experiments and the time elapsed between the images is $\approx$ 10 h.

These STM images show that the interface Au(111)/[$Py_{1,4}$]FAP is complex and more or less featureless at electrode potentials positive from the ocp. The high quality of the liquid, with all impurities present at below 10 ppm, and the recovering of the original gold surface after an anodic step up to +2 V make it unlikely that the STM experiment shows anything else other than the true potential dependent interaction of the IL with the gold surface. We must clearly say that the image quality shown in this study is far away from what is known in aqueous solutions or from other studies of our own in the cathodic regime, which is a consequence of the IL being adsorbed on the electrode surface quite strongly. The STM tip interacts with this layer of strongly bound ions: this complicated interface results in STM images of lower quality than might be expected in aqueous solutions. In our opinion, this will be the challenge with *in situ* STM experiments using ILs; detailed analysis of different liquids is necessary to shed more light on the potential and liquid dependent interface electrode(s)/ionic liquid(s).

In the last section of this paper we would like to present our first results on the influence of solutes on the interface structure Au(111)/[$Py_{1,4}$]FAP. In reference 23 we reported that the electrodeposition of tantalum in 1-butyl-1-methylpyrrolidinium bis(trifluoromethylsulfonyl)amide ([$Py_{1,4}$]TFSA) from TaF_5 is easier if LiF is added to the IL and an influence of LiF on the interface could not be excluded as an explanation. Stimulated by this experiment we added — for a first approach — 10 wt% of LiCl to the same extremely pure [$Py_{1,4}$]FAP. Fig. 11a shows the typical AFM force distance curve of [$Py_{1,4}$]FAP/Au(111) at the open circuit potential. The results are identical to the ones published before. However, if 10 wt% of LiCl is added to the liquid the situation is drastically changed at the open circuit potential, Fig. 11b. We still see 5 ion pair steps, each $\sim$0.9 nm wide, but there is no clear repulsive

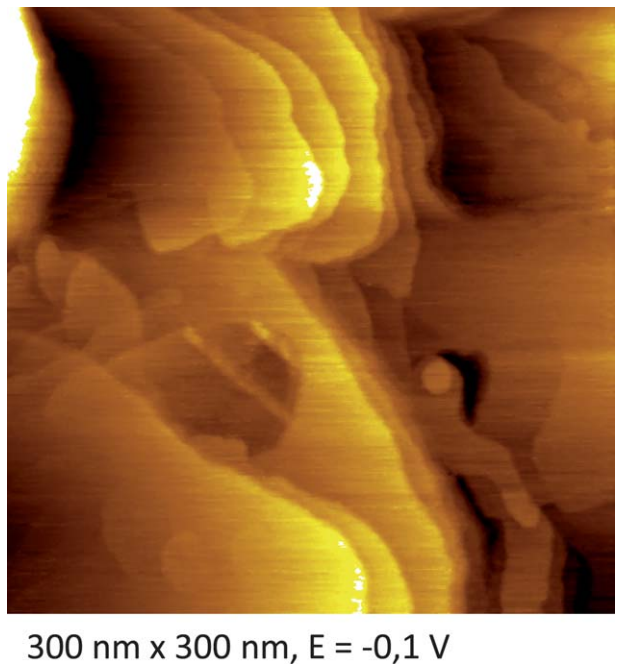

Fig. 10 *In situ* STM image of Au(111)/[$Py_{1,4}$]FAP set back to the former ocp. The original gold surface is recovered.

step at the surface before the AFM tip touches the gold surface. Rather the force has become attractive, and a jump to contact occurs starting ≈ 2 nm from the surface, reminiscent of data obtained previously for the pure ethylammonium nitrate–graphite system[18] or when water was added.[24,25] The forces are attractive and there is jump into contact through the final layer. Fig. 11c is an overlay of both curves showing the considerably different behaviour. Although 10% of LiCl seems to be quite high at the first glance, such a concentration is close to that which would be feasible *e.g.* for an IL based battery electrolyte, and it has to be expected that solutes (and impurities) strongly alter the interface structure. A detailed picture of the interface processes in the presence of solutes will require experiments with different concentrations of solutes at different electrode potentials. However, these preliminary experiments suggest that the added inorganic ions are preferentially located immediately adjacent to the electrode surface, as the structure of the layer farther from the surface (*i.e.* beyond 2 nm) appears largely unaffected, with the number of steps and rupture force the same. The inorganic ions appear to weaken the near surface IL nanostructure, possibly by disrupting solvophobic interactions between cation alkyl chains,[26] such that the van der Waals attractions between the tip and surface dominate. This produces a jump to contact. An alternative explanation is that the level of structure remains constant, but that the Hamaker constant increases in the vicinity of the surface. In either case, the fact that the steps in the force curve are present through the jump to contact means that substantial near surface structure remains.

An *in situ* STM study of the Li underpotential deposition in [$Py_{1,4}$]TFSA containing 0.5 mol L^{-1} LiTFSA showed, compared to the pure IL, a considerably different surface behavior on Au(111), and hints at a Solid Electrolyte Interface where the image quality in the STM experiment was altered.[27] The results presented here show without doubt that solutes can strongly alter the ionic liquid(s)/electrode(s)

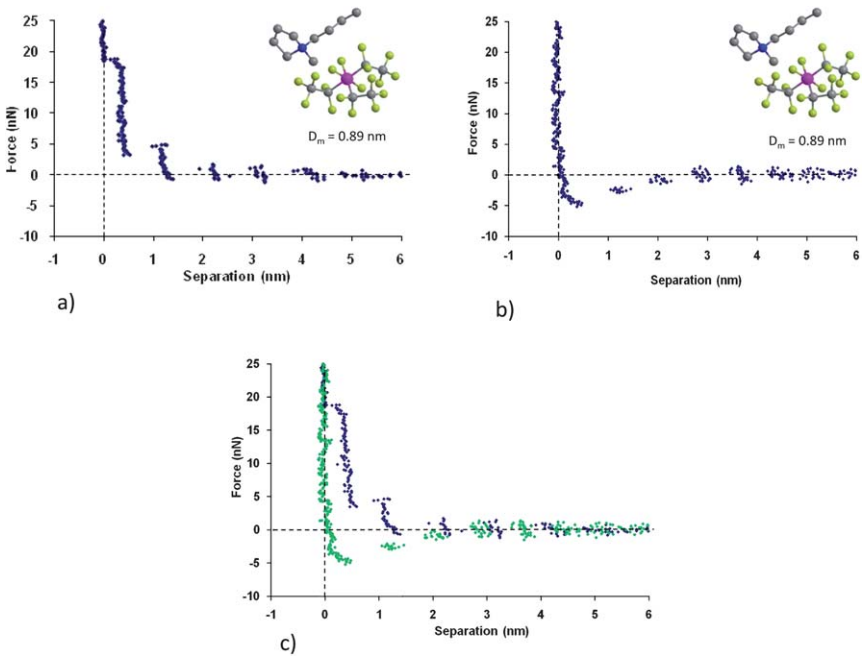

Fig. 11 AFM force/distance profiles of Au(111)/[$Py_{1,4}$]FAP (a) and of Au(111)/[$Py_{1,4}$]FAP with 10 wt% of LiCl (b). The addition of LiCl changes the force profile from repulsive to attractive, thus the interface structure is strongly altered. c) shows both curves overlayed.

interface, and it has to be expected that these effects vary with liquid, solute, solute concentration, electrode, and temperature. In order to get a fundamental picture of electrochemical processes in ionic liquids a combination of electrochemical and *in situ* STM/AFM experiments will be required.

Conclusions

In this paper we have presented our recent results on the interface Au(111)/[$Py_{1,4}$] FAP, probed with the *in situ* STM at electrode potentials more positive than open circuit potential. In contrast to the cathodic regime, where we were able to probe the "famous" herringbone superstructure of Au(111) in a limited potential regime with the STM, the image quality is much lower in the anodic regime, where AFM data suggest surface adsorption of the FAP anion. Nevertheless, it is clearly visible that a layer forms on top of the gold surface with maximum height differences of $\approx$ 0.6 nm. The combination of STM and AFM data reveals that the structure of this layer is not uniform and might be a mixture of cations and anions around +1 V. At +1.8 V a smooth surface is probed by the STM, and the steps between different terraces appear buried under an anion-rich layer. When the electrode potential is set back to the ocp the original gold surface is recovered, thus the adsorption/desorption of the ions seems to be reversible. The observed processes all occur very slowly over several hours.

We conclude that an *in situ* STM investigation of this liquid on Au(111) is not trivial and will require careful adjustment of tunneling parameters. Preliminary results on the addition of solutes (10 wt% of LiCl) to [$Py_{1,4}$]FAP reveal that the near surface structure at the open circuit potential is considerably altered. Instead of repulsive forces, attractive forces are measured, which must influence the STM experiment and more generally, it appears that dissolved solutes will substantially influence IL interface electrochemistry. At a minimum we can conclude that the situation for ionic liquids is much more complicated than the situation for aqueous solutions.

Acknowledgements

This work was financially supported by the Deutsche Forschungsgemeinschaft (DFG) within the Priority Program SPP 1191 - Ionic Liquids and by an Australian Research Council Discovery Project (DP0986194). R.H. thanks the University of Newcastle for a PhD stipend.

References

1 M. Armand, F. Endres, D. R. MacFarlane, H. Ohno and B. Scrosati, *Nat. Mater.*, 2009, **8**, 621.
2 M. V. Fedorov and A. A. Kornyshev, *J. Phys. Chem. B*, 2008, **112**, 11868.
3 M. V. Fedorov and A. A. Kornyshev, *Electrochim. Acta*, 2008, **53**, 6835.
4 S. A. Kislenko, I. S. Samoylov and R. H. Amirov, *Phys. Chem. Chem. Phys.*, 2009, **11**, 5584.
5 V. Lockett, R. Sedev, J. Ralston, M. Horne and T. Rodopoulos, *J. Phys. Chem. C*, 2008, **112**, 7486.
6 T. R. Gore, T. Bond, W. Zhang, R. W. J. Scott and I. J. Burgess, *Electrochem. Commun.*, 2010, **12**, 1340.
7 M. V. Fedorov, N. Georgi and A. A. Kornyshev, *Electrochem. Commun.*, 2010, **12**, 296.
8 M. Z. Bazant, B. D. Storey and A. A. Kornyshev, *Phys. Rev. Lett.*, 2011, **106**, article number 046102.
9 R. Atkin and G. G. Warr, *J. Phys. Chem. C*, 2007, **111**, 5162.
10 M. Mezger, H. Schröder, H. Reichert, S. Schramm, J. S. Okasinski, S. Schröder, V. Honkimäki, M. Deutsch, B. M. Ocko, J. Ralston, M. Rohwerder, M. Stratmann and H. Dosch, *Science*, 2008, **322**, 424.
11 R. Atkin, S. Zein El Abedin, R. Hayes, L. H. S. Gasparotto, N. Borisenko and F. Endres, *J. Phys. Chem. C*, 2009, **113**, 13266.

12 S. J. O'Shea, M. E. Welland and J. B. Pethica, *Chem. Phys. Lett.*, 1994, **223**, 336.
13 R. Lim and S. J. O'Shea, *Langmuir*, 2004, **20**, 4916.
14 S. Jeffery, P. M. Hoffmann, J. B. Pethica, C. Ramanujan, H. O. Ozer and A. Oral, *Phys. Rev. B: Condens. Matter Mater. Phys.*, 2004, **70**, 054114.
15 F. Endres, O. Höfft, N. Borisenko, L. H. S. Gasparotto, A. Prowald, R. Al-Salman, T. Carstens, R. Atkin, A. Bund and S. Zein El Abedin, *Phys. Chem. Chem. Phys.*, 2010, **12**, 1724.
16 R. Atkin, N. Borisenko, M. Drüschler, S. Zein El Abedin, F. Endres, R. Hayes, B. Huber and B. Roling, *Phys. Chem. Chem. Phys.*, 2011, **13**, 6849, DOI: 10.1039/c0cp02846k.
17 F. Endres, S. Zein El Abedin and N. Borisenko, *Z. Phys. Chem.*, 2006, **220**, 1377.
18 R. Hayes, G. G. Warr and R. Atkin, *Phys. Chem. Chem. Phys.*, 2010, **12**, 1709.
19 D. Wakeham, R. Hayes, G. G. Warr and R. Atkin, *J. Phys. Chem. B*, 2009, **113**, 5961.
20 R. Hayes, S. Zein El Abedin and R. Atkin, *J. Phys. Chem. B*, 2009, **113**, 7049.
21 B. R. Clare, P. M. Baylay, A. S. Best, M. Forsyth and D. R. MacFarlane, *Chem. Commun.*, 2008, 2689.
22 R. Hayes, N. Borissenko, M. K. Tam, P. C. Howlett, F. Endres and R. Atkin, J. Phys. Chem. C , DOI: 10.1021/jp200544b.
23 S. Zein El Abedin, H. K. Farag, E. M. Moustafa, U. Welz-Biermann and F. Endres, *Phys. Chem. Chem. Phys.*, 2005, **7**, 2333.
24 J. Smith, O. Werzer, G. B. Webber, G. G. Warr and R. Atkin, *J. Phys. Chem. Lett.*, 2010, 1.
25 R. G. Horn, D. F. Evans and B. W. Ninham, *J. Phys. Chem.*, 1998, **92**, 3531.
26 R. Hayes, S. Imberti, G. G. Warr and R. Atkin, *Phys. Chem. Chem. Phys.*, 2011, **13**, 3237.
27 L. H. S. Gasparotto, N. Borisenko, N. Bocchi, S. Zein El Abedin and F. Endres, *Phys. Chem. Chem. Phys.*, 2009, **11**, 11140.